Omicron vs. the Rest: Assessing the Competitive Dynamics and Coinfection Scenarios of COVID-19 Strains on a Social Network

Hamed Jabraeilian, Yousef Jamali*

Department of Applied Mathematics, Tarbiat Modares University, Tehran, Iran

Abstract

The rapid spread and evolving nature of COVID-19 variants have raised concerns regarding their competitive dynamics and coinfection scenarios. In this study, we assess the competitive interactions between the Omicron variant and other prominent variants (Alpha, Beta, and Delta) on a social network, considering both single infection and coinfection states. Using the SIRS model, we simulate the progression of these variants and analyze their impact on infection rates, mortality, and overall disease burden. Our findings demonstrate that the Alpha and Beta strains exhibit comparable contagion levels, with the Alpha strain displaying higher infection and mortality rates. Moreover, the Delta strain emerges as the most prevalent and virulent strain, surpassing the other variants. When introduced alongside the less virulent Omicron strain, the Delta strain results in higher infection and mortality rates. However, the Omicron strain's dominance leads to an overall increase in disease statistics. Remarkably, our study highlights the efficacy of the Omicron variant in supplanting more virulent strains and its potential role in mitigating the spread of infectious diseases. The Omicron strain demonstrates a competitive advantage over the other variants, suggesting its potential to reduce the severity of the disease and alleviate the burden on healthcare systems. These findings underscore the importance of monitoring and understanding the dynamics of COVID-19 variants, as they can inform effective prevention and mitigation strategies, particularly with the emergence of variants that possess a relative advantage in controlling disease transmission.

Keywords: Virulence, Transmissibility, Coinfection, Competition

1. Introduction

The understanding of epidemics plays a crucial role in comprehending disease spread models and developing effective strategies to prevent the over-infection of populations. In this context, the significance of mathematical models cannot be overlooked in the field of epidemiology.

The virulence of a pathogen refers to the mortality rate caused by the disease [1]. Virulence and disease transmissibility are key factors in the investigation of disease models.

Multi-infection models encompass the simultaneous spread of several independent viruses within a community. The various types of multiple infections include single infection, coinfection and superinfection. In the case of single infection, when a strain spreads independently among a population of susceptible individuals, an infected person will only harbor that specific strain until recovery, without contracting another strain. This scenario is termed single infection. Superinfection models account for the possibility of an infected individual being susceptible to multiple strains of the disease simultaneously, with a more virulent strain potentially replacing a less virulent strain through a process akin to hostile takeover [2, 3]. Coinfection models involve individuals sustaining infections with multiple

pathogen strains concurrently [4, 5], although typically, susceptible individuals do not contract more than one infection at a time.

In recent years, the COVID-19 epidemic has witnessed the emergence of various variants [6] as reported by the World Health Organization (WHO). A change in the genetic sequence of a virus is referred to as a mutation and variants are genomes that differ from each other in terms of their genetic sequence, often resulting from one or more mutations [7]. As a single-stranded RNA virus [8], SARS-CoV-2 has undergone numerous mutations. While most mutations do not significantly impact the virus's spread and mortality, several mutations have raised global concerns. Hence, it is crucial to develop a better understanding of the transmission of these new coronavirus variants and effective methods to mitigate their spread [9, 10]. Compared to the original lineage, new coronavirus variants exhibit higher transmissibility and increased resistance to antibodies [11].

To prioritize surveillance and research on these variants, the WHO has categorized COVID-19 strains into three groups: variants of interest (VOI), variants of concern (VOC) and variants under monitoring (VUM). The classification of variants may vary across different countries[12]. The four previous VOCs include Alpha (B.1.1.7), Beta (B.1.351), Gamma (P.1) and Delta (B.1.617.2). All of these variants have triggered new waves of epidemics worldwide. On November 26, 2021, the WHO designated a new variant called Omicron (B.1.1.529) as the fifth VOC, instantly sparking global concerns [6]. The term "Wild type" refers to a virus or background strain that does not possess any major mutations [13]. In other words, it represents the natural, non-mutated strain of the virus [14]. The transmission and virulence rates for the main strain, referred to as the Wild type, are based on reference [15].

The main concerns regarding SARS-CoV-2 VOCs encompass viral transmission, disease severity and their effects on vaccine efficacy [16]. The Wild type virus of COVID-19 is more susceptible to neutralization compared to newer variants [17]. According to a study, the Alpha strain exhibited a 43% to 90% higher transmissibility than the Wild type [18]. Additionally, the Alpha lineage demonstrated a 71% higher transmission rate compared to the original lineage [19]. Generally, the Delta and Omicron variants are more transmissible than the Alpha, Beta and Gamma variants [17].

Quantitatively speaking, the Delta variant posed a 108% increased risk of hospitalization, a 235% increased risk of ICU admission and a 133% higher risk of death compared to the original variant [20]. Another study reported that the Delta strain was 60% more transmissible than the Alpha strain, becoming the dominant strain as of August 2021 [21]. Analysis by Bolze et al. revealed that the Delta variant exhibited, on average, 1.7 times higher viral load compared to the Alpha variant [22]. Furthermore, according to another report, the transmissibility of the Delta strain is usually 60% higher than that of the Alpha strain, making it the most infectious variant to date and 97% more contagious than the original strain [23]. Similarly, the Beta strain is 50% more transmissible than the Wild type [24]. Data also indicate that the Delta variant has a higher transmission rate than the Gamma variant [25], with the estimated transmission capability of the Gamma variant being 2.6 times higher than that of the Wild type, according to reference [26]. A report from Public Health England on June 11 indicated a significantly higher risk of hospitalization associated with the Delta variant compared to the Alpha variant [27]. In short, the Delta strain exhibits highly transmissible characteristics and greater invasiveness [28]. Another study highlighted that the infection rates of the Omicron variant

were four times higher than the Wild type and twice as high as the Delta variant [29]. Reference [30] estimates that the Omicron variant is 36.5% more transmissible than the Delta variant. Moreover, a study conducted in Southern California demonstrated that the Omicron strain had a 91% lower fatality rate than the Delta strain and a 51% reduced likelihood of hospitalization [31].

All the VOCs, including Alpha, Beta, Gamma and Delta variants present higher risks of hospitalization, ICU admission and mortality compared to the Wild type virus. Beta and Delta variants pose a higher risk than Alpha and Gamma variants [16]. Alpha, Beta, Gamma and Delta variants had 1.7, 3.6, 2.6 and 2.08 times increased risk of hospitalization, respectively and 2.3, 3.3, 2.2 and 3.35 times increased risk of ICU admission, respectively [16, 32]. These variants also exhibit mortality risks of 1.37, 1.50, 1.06 and 2.33, respectively [16]. The mortality rate of the Alpha strain, as referenced in [33], is reported as 0.005. Qualitatively estimating the transmission and virulence rates for this variant aligns with this reference. Figure 1 illustrates the outcome of our research aimed at investigating the factors influencing the infection, transmission and virulence of COVID-19 variants. All values have been qualitatively investigated, collected and estimated, thus the disease transmission and virulence rates depicted in Figure 1 will be referred to as qualitative rates.

Newer VOCs have largely displaced other circulating SARS-CoV-2 variants. Delta accounted for nearly 90% of all viral sequences submitted to GISAID by October 2021 and Omicron has now become the dominant strain circulating worldwide, representing more than 98% of shared viral sequences in GISAID since February 2022 [34].

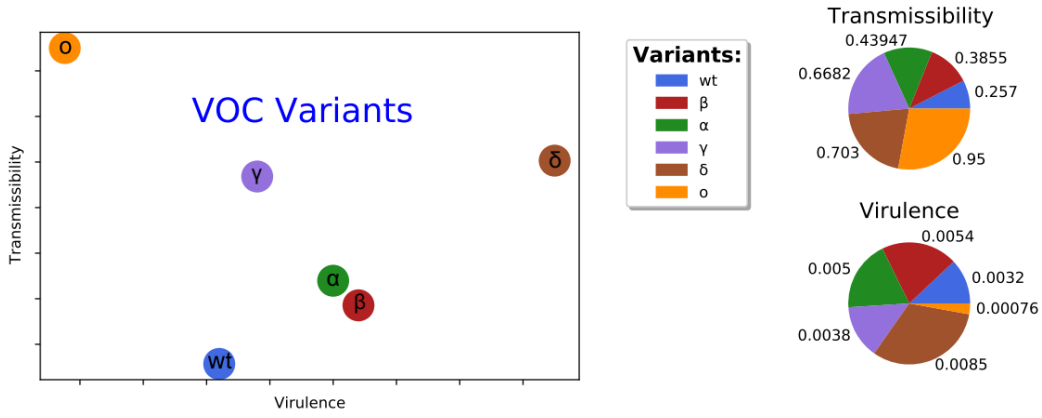

Fig 1. Qualitative plot of different VOC variants of the disease of Covid-19

The simultaneous circulation of multiple variants in the same location can lead to coinfection with different strains of SARS-CoV-2. Yaqing He et al. reported the identification of an individual co-infected with two worrisome SARS-CoV-2 variants, Beta and Delta [35]. Additionally, Deltacron, involving both Delta and Omicron variants, was first detected in January 2022 and rapidly spread in Cyprus [36]. Several recombination events between the main subvariants of Omicron (BA.1 and BA.2) and other variants of concern (VOCs) and variants of interest (VOIs) have been observed [37].

Mathematical models are essential tools for studying the spread of COVID-19 in social networks. Manotosh Mandal et al. introduced the SEQIR model, which considers susceptible (S), exposed (E), infected in hospital (Q), quarantined (I) and recovered or eliminated (R) individuals [38]. Joe Pharaon and Chris T compared the dynamics of a two-strain SIRX compartmental epidemic model with and without adaptive social behavior, where susceptible individuals (S) can be infected by a resident strain (I1) or a mutant strain (I2). The proportion of individuals adopting preventive behaviors is represented by X, referred to as protective behavior [39]. Cleo Anastassopoulou et al. proposed the SIRD model to estimate parameters and predict the spread of the COVID-19 epidemic in Hubei Province, China, using real data [40]. Verónica Miró Pina et al. developed models based on Erdős-Rényi and a power-law degree distribution, which capture the role of heterogeneity and connectivity and can be extended to make hypotheses about demographic characteristics. They demonstrated that changes in the number of contacts in a population impact the effectiveness of public health interventions such as quarantine or vaccination strategies [41]. Pilar Hernández et al. utilized the SEIR model and presented two types of agent-based model simulations: a homogeneous spatial simulation where contamination occurs through proximity and a model in a scale-free network with different clustering characteristics, where contamination occurs between any two agents through their link, if any [42]. Mosquera and Adler established consistency conditions on the parameters of a mathematical model for coinfection states, including superinfection as a limit of the coinfection model and a special single infection state [43].

In this manuscript, we present the SIRS model as an extension of the framework developed by Mosquera and Adler. Our study entails a comprehensive analysis and discussion of simulations conducted on a social network, incorporating both single infection and coinfection states. With a specific emphasis on the emerging variants of COVID-19, we explore the intricate dynamics of strain competition within the contexts of single infection, coinfection and delayed states. Furthermore, we thoroughly investigate the influence of network topology on the overall progression of the epidemic.

2. Model

We investigate the scenario of multiple infections by considering a simplified case where only one or two infectious diseases can occur concurrently within the population. In the context of the SIRS model applied to the network, we mathematically describe the dynamics of the epidemic. Consequently, the network consists of four distinct agent types: susceptible individuals (S), individuals infected with virus strain 1 (I_1), individuals infected with virus strain 2 (I_2) and individuals simultaneously infected with both strains (I_{12}). Notably, the susceptible class is further categorized into two groups: susceptible individuals 1 (S_1) who have not been infected and are susceptible to receiving the infection and susceptible individuals 2 (S_2) who have previously experienced an infectious disease but remain susceptible with a lower probability.

Examining the impact of mask usage on COVID-19 transmission, a study directly analyzed its effect within the community. The findings revealed that if face masks were universally worn within a household before symptom onset, they effectively reduced transmission by 79% [44]. Masks play a crucial role in preventing the spread of droplets and aerosols emitted by infected individuals [45]. Correct usage of surgical masks can significantly decrease virus transmission by approximately 95%, providing around 85% protection against infection for non-infected

individuals [46]. Furthermore, another study identified mental health status and social media as factors influencing adherence to social distancing measures. The high compliance rate of social distancing measures was reported by the majority of respondents (95.6%) [47]. Thus, assuming adherence to health protocols such as mask-wearing, social distancing and other preventive measures against COVID-19 transmission, we define the protection parameter (p) as the reduction in the probability of infection transmission. In light of the aforementioned cases, we set the protection parameter to $p = 0.9$.

2.1. Coinfection model

In order to define the coinfection model, we make the following assumptions:

1. The mortality rate of individuals due to non-disease factors during the simulation interval can be neglected.

2. Infected individuals with strain i recover at a rate of γ_i and have a mortality rate of δ_i attributed to the infection. They are then classified as removed (R).

3. Individuals infected with both strains simultaneously experience a disease-related mortality rate of δ_{12}. These individuals recover from strain 1 viral disease at a rate of γ_{21}, while co-infected individuals recover from strain 2 viral disease at a rate of γ_{12}.

4. Susceptible individuals become infected by individuals infected with strains 1 and 2 at rates of β_1 and β_2, respectively.

5. The transmissibility rate for individuals co-infected with both strains can differ from the rate for individuals infected with strains 1 and 2 separately. Specifically, if the reduced infectiousness of co-infected individuals acting as strain i is denoted by ϵ_i, the rate at which susceptible individuals acquire strain i from co-infected individuals will be $\epsilon_i\beta_i I_{12}$, where ϵ_i belongs to the range [0, 1]. This means that when a susceptible individual interacts with a co-infected individual, the transmission of either I_1 or I_2 disease (depending on the competition between strains) occurs at a lower rate.

6. If there is reduced susceptibility to the other strain when infected with strain i, denoted by a_i, the infection rate of I_1 individuals by strain 2 is less than the infection rate of susceptible individuals by a factor of a_2. Similarly, the infection rate of I_2 individuals by strain 1 is equal to $a_1\beta_1 I_1 + a_1\varepsilon_1\beta_1 I_{12}$.

7. In the case of reinfection, susceptible individuals 2 (S_2) contract strain i at a much lower transmission rate of $\alpha\beta_i$.

Based on these assumptions, the coinfection model follows the set of equations below, where the total number of individuals in the network is denoted as $N = S_1+S_2+I_1+I_2+I_{12}+R$.:

$$\frac{dS_1}{dt} = -(1-p)\{\beta_1 I_1 S_1 + \beta_2 I_2 S_1 + \epsilon_1\beta_1 I_{12} S_1 + \epsilon_2\beta_2 I_{12} S_1\}$$

$$\frac{dS_2}{dt} = -\alpha(1-p)\{\beta_1 I_1 S_2 + \beta_2 I_2 S_2 + \epsilon_1\beta_1 I_{12} S_2 + \epsilon_2\beta_2 I_{12} S_2\} + \gamma_1 I_1 + \gamma_2 I_2$$

$$\frac{dI_1}{dt} = (1-p)\beta_1(S_1 + \alpha S_2)(I_1 + \epsilon_1 I_{12}) - (\delta_1 + \gamma_1)I_1 - a_2\beta_2 I_1 I_2 + \gamma_{12} I_{12} - \epsilon_2 a_2 \beta_2 I_1 I_{12}$$

$$\frac{dI_2}{dt} = (1-p)\beta_2(S_1 + \alpha S_2)(I_2 + \epsilon_2 I_{12}) - (\delta_2 + \gamma_2)I_2 - a_1\beta_1 I_1 I_2 + \gamma_{21} I_{12} - \epsilon_1 a_1 \beta_1 I_2 I_{12}$$

$$\frac{dI_{12}}{dt} = (a_1\beta_1 + a_2\beta_2)I_1 I_2 + (\epsilon_2 a_2 \beta_2 I_1 + \epsilon_1 a_1 \beta_1 I_2)I_{12} - (\gamma_{12} + \gamma_{21} + \delta_{12})I_{12}$$

$$\frac{dR}{dt} = \delta_1 I_1 + \delta_2 I_2 + \delta_{12} I_{12} \quad (1)$$

Generally, Figure 2 illustrates the set of equations (1) that represent the coinfection model:

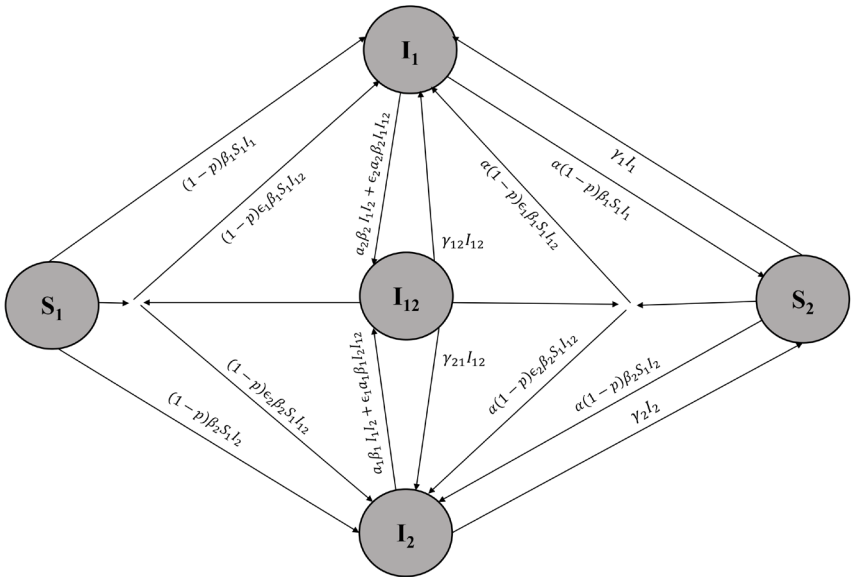

Fig 2. Schematic diagram illustrating the interaction between two different strains in the coinfection model. Susceptible individuals S_1 can become infected by interacting with infectious individuals I_1 and I_{12} at rates β_1 and $\epsilon_1\beta_1$, respectively. If they have protection, they are transferred to the I_1 class with a coefficient of (1-p). Infectious individuals I_1 can transition to the I_{12} class by interacting with infectious individuals I_2 and I_{12} at rates $a_2\beta_2$ and $\epsilon_2 a_2\beta_2$, respectively. Individuals in the I_1 class are removed at a rate of δ_1 and recover at a rate of γ_1, transitioning to the S_2 class. The process is similar for susceptible individuals S_2, but at a much lower rate. The same interactions and transitions apply to individuals in the I_2 class as well.

2.2 Single infection model

In the single infection model, infected individuals are not susceptible to further infection. By setting the coinfection coefficient equal to zero ($a_1 = a_2 = 0$), which implies that $I_{12} = 0$, the dynamic terms of the coinfection model are simplified, resulting in the following model:

$$\frac{dS_1}{dt} = -(1-p)\{\beta_1 I_1 S_1 + \beta_2 I_2 S_1\}$$

$$\frac{dS_2}{dt} = -\alpha(1-p)\{\beta_1 I_1 S_2 + \beta_2 I_2 S_2\} + \gamma_1 I_1 + \gamma_2 I_2$$

$$\frac{dI_1}{dt} = (1-p)\beta_1(S_1 + \alpha S_2)I_1 - (\delta_1 + \gamma_1)I_1$$

$$\frac{dI_2}{dt} = (1-p)\beta_2(S_1 + \alpha S_2)I_2 - (\delta_2 + \gamma_2)I_2$$

$$\frac{dR}{dt} = \delta_1 I_1 + \delta_2 I_2 \qquad (2)$$

For the model implementation, we adopt an Erdős–Rényi random network with a total of N = 10,000 nodes and an average degree of k = 10. The simulation is conducted for a specified time interval T and each run is repeated 50 times for reliable results.

To examine the competition and coinfection dynamics between different strains, we consider the rates associated with the Covid-19 epidemic. It is important to note that in each simulation, the presence of two strain types in the community is taken into account. Table 1 presents the parameter values for various models of Covid-19, which are derived from ten different references [15, 39, 48-55]. Notably, the units in the table are given in terms of per day (day^{-1}). To incorporate real-world data, we refer to reference [15] for the parameters related to the Wild type of the virus.

Table 1. Values of parameters of various models of Covid-19

Models	β	γ	δ	references
SIR	0.4	0.2	0.05	[39]
SIRD	0.21542	0.017129	0.011832	[48]
SIRD	0.257	0.0315	0.0032	[15]
SAIU	0.274	-	-	[49]
SIQR	0.13	0.15	0.038	[50]
SEIR	-	-	0.0018	[51]
SEIR	0.29	0.09722	-	[52]
SEAIR	-	0.13978	0.015	[53]
SEIAHRD	0.38974	0.1428	0.015	[54]
SEAIQHR	1.11525	0.01496	0.04142	[55]

3. Results and Discussion

In our study, we focused on the variants of Covid-19, specifically the Alpha, Beta, Delta and Omicron strains. By utilizing the findings of our research, we conducted simulations to examine the dynamics of these strains.

3.1 Investigating the competition between covid-19 variants with strain rates

We began by considering the single infection state for the four VOC strains and observed their dynamic changes during the epidemic, as shown in Figure 3. The contagion of the Alpha and

Beta strains was relatively similar, with the Alpha strain exhibiting approximately 5% more cases than the Beta strain. However, compared to the Wild type, the Alpha strain had a peak infection and mortality rate almost twice as high. Furthermore, the Delta strain exhibited a higher prevalence of disease and mortality compared to the other three strains. We also examined the competition between strains in the following scenarios:

1) Competition between the Wild type and the Alpha variant
2) Competition between the Alpha and the Beta variants
3) Competition between the Delta and the Omicron variants

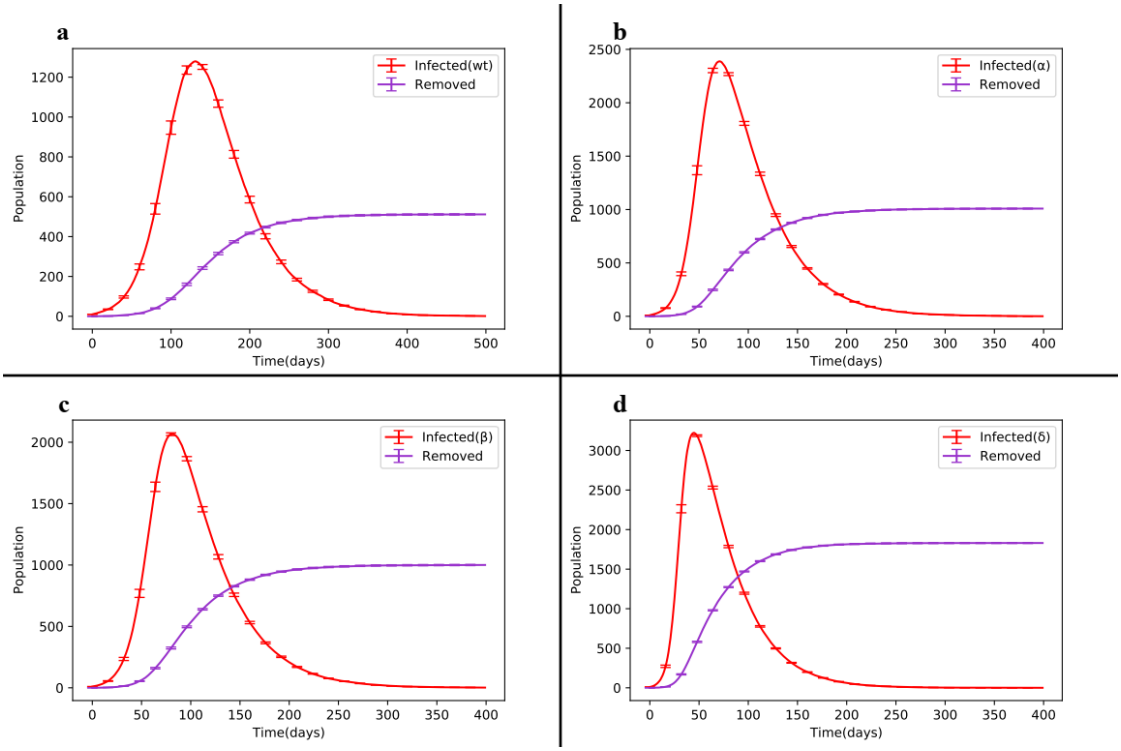

Fig 3. Dynamic changes of the SIRS model in the single infection state. (a) Outbreak of the Wild type. (b) Outbreak of the Alpha variant. (c) Outbreak of the Beta variant. (d) Outbreak of the Delta variant in the Erdős–Rényi network.

Initially, we evaluated the Wild type and the Alpha mutant variant in a society with a size of N=10,000. As depicted in Figure 4-a, the number of infected individuals for the main strain and the Alpha strain reached their maximum values after t=59 days (I1max=109) and t=73 days (I2max=2199), respectively. By t=200 days, the number of infected individuals for the main strain decreased to 4, while for the Alpha strain, it was 167. It is worth noting that the mutated Alpha strain had a wider epidemic range and resulted in a significantly higher number of infections compared to the original strain. The number of individuals who experienced either the main strain or the Alpha strain at least once was 3.21% and 68.50%, respectively.

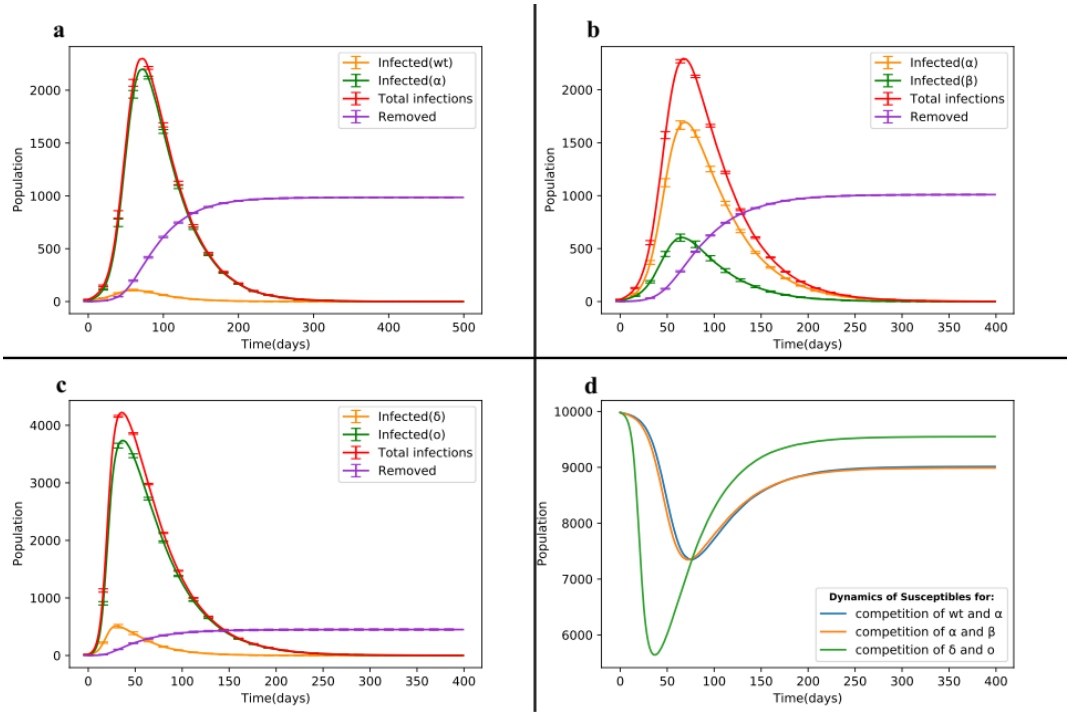

Fig 4. Dynamic changes of the SIRS model in the competition between strains. (a) Competition between the Wild type and Alpha mutant strain. (b) Competition between Alpha and Beta strains. (c) Competition between Delta and Omicron strains. (d) Dynamics changes of susceptible individuals.

In Figure 4-b, the total number of Covid-19 cases through the Alpha strain was nearly 2.8 times higher than that of the Beta strain. The key difference between Figure 4-b and Figure 4-a is that the Beta strain replaced the main strain and the overall number of infected individuals was distributed in a ratio of 3 to 1. An important concern arises when two highly transmissible strains enter the community. Thus, we introduced the more virulent Delta variant and the less virulent Omicron variant into the network and their interaction among nodes yielded the dynamics of infected individuals as shown in Figure 4-c.

The total number of infections for the Delta and Omicron strains was 11.54% and 89.96%, respectively. The mortality rate due to the disease was higher for the Delta strain, as its virulence was 91% greater than that of the Omicron strain. Even though the recovery rates were assumed to be the same for both strains, the number of deaths through the Delta and Omicron strains was 24.3% and 20.8%, respectively. It is important to note that the majority of deaths occurred as a result of the Delta strain.

If we consider the time to reach the peak of the disease (t_{max}), we observe that it is almost half the time in Figure 4-c compared to Figures 4-a and 4-b. This is the reason why these strains are of concern to the World Health Organization (WHO). Due to their higher prevalence, a greater number of susceptible individuals are affected by the disease in a shorter period of time, resulting in a 28.33% increase in the number of infected individuals compared to the previous scenario. The dynamic curve of susceptible individuals in the competition between wt and α strains with α and β strains is similar. However, as depicted in Figure 4-d, when competing Delta and Omicron strains are involved, a larger number of susceptible individuals are affected by the disease. The difference in the minimum points between the previous two cases and the third case is 17.04%. This suggests that the virulence of both strains was higher in the previous two cases, but over time, the equilibrium point of susceptible individuals in the third case is 5.6% lower than that in the other two cases. Table 2 provides detailed information on these three cases for the competition of Covid-19 strains.

Table 2. Statistics of the results obtained for the SIRS model, in the state of competition different strains of Covid-19

Quantity	Description	State1	State2	State3
I_{1max}	Peak domain of dynamics of infected individuals to strain 1	109	1692	513
I_{2max}	Peak domain of dynamics of infected individuals to strain 2	2199	606	3735
I_{1avg}	The total mean of dynamics of infected individuals to strain 1	19	365	70
I_{2avg}	The total mean of dynamics of infected individuals to strain 2	3790	126	685
S_{min}	The minimum value of dynamics of susceptible individuals at the peak of the disease	7346	7345	5642
Total Infected	The total stats of infected individuals to disease	7369	7317	10150
Total Recovered	The total stats of recovered individuals from disease	6384	6306	9698
Total Removed due to infection	The total stats of removed individuals from disease	985	1010	451

Based on the findings from Figure 3 and Figure 4, we can conclude that even if the transmissibility of a strain is approximately 70% higher than the other strain, most of the disease statistics in the society will often be attributed to the strain with the higher transmission rate (as seen in Figures 4-a and 4-b). Additionally, due to the higher transmission and virulence rates of the Delta strain compared to the Wild type, Alpha and Beta strains, the introduction of the Omicron strain, despite its lower virulence, resulted in more disease statistics compared to all the other strains. Therefore, this situation is a cause for concern in terms of increasing the overall disease burden, but it could also be seen as a positive scenario for the removal of a more dangerous strain from the society.

3.2. The delayed state of competition of Covid-19 strains

In this section, we explore the competition between the Wild type-Omicron and Alpha-Omicron strains in a delayed state. In this scenario, the main strain initially spreads in the network and after a certain period, the second strain is introduced. Figures 3-a and 3-b depict the outbreak of the disease through the main and Alpha strains, respectively. The Alpha strain exhibits twice the mortality rate and peak infection level compared to the main strain. Our goal is to introduce a strain with a higher transmission rate into the network with a delay.

In Figure 5-a, we introduce the less virulent Omicron strain when the main strain is in its maximum growth trend (maximum slope). In Figure 5-c, we insert the second strain before the maximum slope of the first strain. As observed in Figures 5-a and 5-c, the addition of the less virulent Omicron strain, with a higher prevalence compared to the main and Alpha strains (4.6 and 4.8 times, respectively), results in a greater number of disease cases. In other words, the Omicron strain effectively suppresses the more virulent strains, acting as a vaccine-like agent. This process continues until the end of the epidemic. Consequently, as shown in Figure 5, the

dynamics of deaths are significantly lower in parts a and c, primarily due to the predominance of the Omicron strain.

It is noteworthy that the second strain must have a higher transmission rate to effectively counteract the more virulent strains. Some experts suggest that Omicron may act as a natural vaccine since it shares certain similarities with weakened live vaccines[56]. Studies have shown that individuals infected with Omicron exhibit a significant immune response that can neutralize not only Omicron but also other variants of concern, including the prevalent Delta variant [57].

If we introduce the second strain during the peak of infected individuals with the Alpha strain, as shown in Figures 5-b and 5-d, the Omicron strain fails to surpass the previous strain with higher transmissibility. The Wild type and Alpha strains, which are more contagious and fatal than the Omicron strain, result in 1.7 and 55 times more disease cases, respectively. Since the Alpha strain has infected a larger portion of the population, leading to more individuals entering the S_2 class, the Omicron strain struggles to infect these individuals effectively. Consequently, the dynamics of infected individuals to the second strain appear almost as a straight line.

Overall, the delayed introduction of the less virulent Omicron strain can significantly reduce the disease burden caused by more virulent strains, highlighting its potential role as a protective factor against the spread of highly contagious variants.

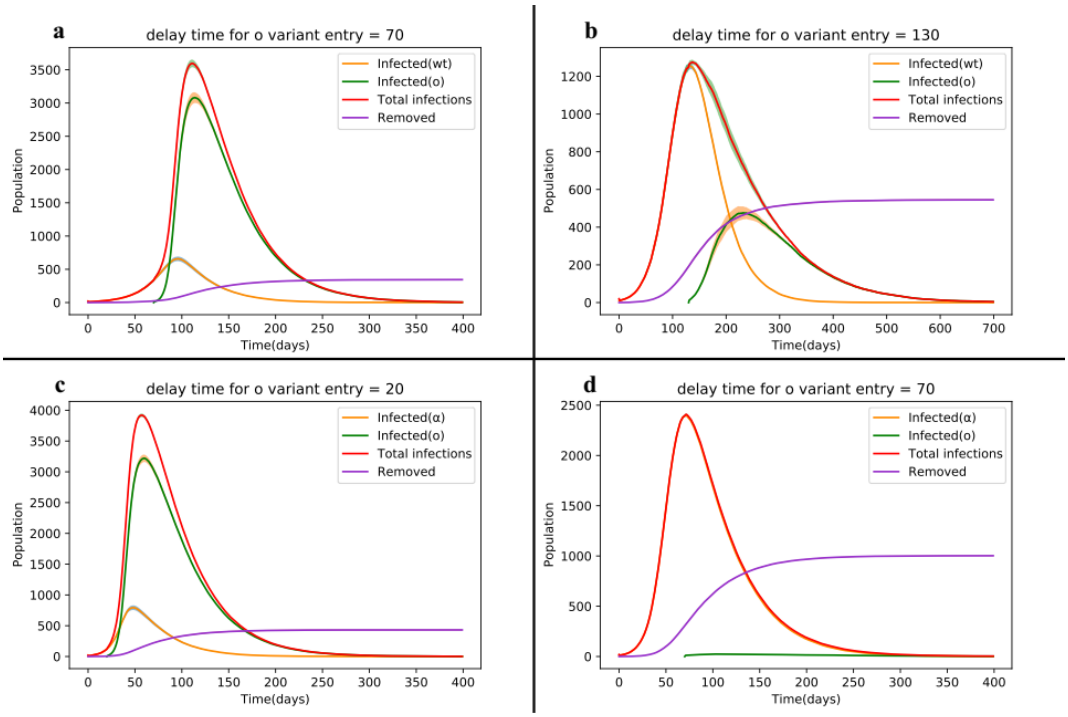

Fig 5. Delay state diagram depicting the dynamic changes of the SIRS model during the competition between the Wild type, Alpha and Omicron strains. The colored hachure in the peak of the curves represents the error bars for 50 times experiments in each run.

3-.3. Investigating coinfection between covid-19 variants

In this section, we examine the coinfection dynamics between the Delta and Omicron strains, collectively referred to as Deltacron, by analyzing the behavior of co-infected individuals for different values of parameter a, specifically a = 0.1, 0.5, 1 and 2.

When considering values of a < 1 (see Figure 6), which correspond to lower levels of coinfection, we observe that the dynamics of infected individuals for the Delta strain reaches its peak 10 days earlier than that of the Omicron strain. This can be attributed to the weaker co-infectious conversion between infected individuals of the Omicron and Delta strains, resulting in a lower rate of conversion and the earlier peak for the Delta strain due to its higher virulence.

There are two noteworthy observations in this scenario. Firstly, the slope reduction between the interval [50, 100] for the Delta strain dynamics is more significant for a = 0.1 compared to a = 0.5. This reduction becomes smoother as the presence of co-infected individuals increases and they transition to classes I_1 and I_2. For example, the slope decreases from -5.6 for a = 0.1 to -3.8 for a = 0.5 in this interval.

Secondly, as the coefficient a increases, the dynamics of co-infected individuals show an overall increase. Despite the Omicron strain being dominant, the shape of the Delta strain dynamics differs before reaching its peak (see Figures 5-c and 5-d). For instance, when a = 1 in the interval [10, 20], all three dynamics initially exhibit an increasing trend, with the share of coinfection through the Delta strain being approximately 20% higher than that of Omicron. This is due to the random network structure and the interaction between infected individuals of both strains, where the Delta strain has a higher chance of selection for coinfection. Over time, as the Omicron strain becomes more prevalent, it gradually surpasses the Delta strain, reaching its peak at t = 32. In the interval [20, 32], the share of coinfection through the Omicron strain becomes greater than that of Delta, leading to a gradual decrease in the dynamics of Delta-infected individuals with a slope of -2. Meanwhile, the dynamics of individuals in class I_1 continue to increase until they reach their peak at t = 51. Moreover, in [32, 51], the Omicron strain is involved in coinfection nearly 60% more than the Delta strain. As the dynamics of class I_2 decline and the dynamics of class I_1 culminate, the dynamics of coinfection align with that of class I_1. From t = 51 onwards, all three dynamics exhibit a decreasing trend. Consequently, higher values of a lead to an earlier peak in the dynamics of infected individuals for the Omicron strain compared to the Delta strain and coinfection. Subsequently, all three curves gradually decline, signifying the end of the epidemic after approximately 250 days.

In general, if individuals in the coinfection class (I_{12}) are rapidly removed, the I_{12} class decreases to zero. The total number of removals, as indicated by relation (1) [43], is given by $\Gamma = \gamma_{12} + \gamma_{21} + \delta_{12}$. Thus, the reduction of co-infected individuals is approximated by the rapid elimination of these individuals through rapid recovery from either strain or by an increase in mortality due to double infection itself. Table 3 provides the results for the four aforementioned cases. It is worth noting that although the network size is $N = 10^4$, the numbers in Table 3 appear larger. For instance, in the case of a = 2, the total number of patients is 23,459, implying that individuals who have had the disease and recovered remain susceptible to reinfection. For this specific case, the number of individuals infected with the Delta, Omicron and Deltacron strains at least once is 2,203, 7,680 and 4,997, respectively.

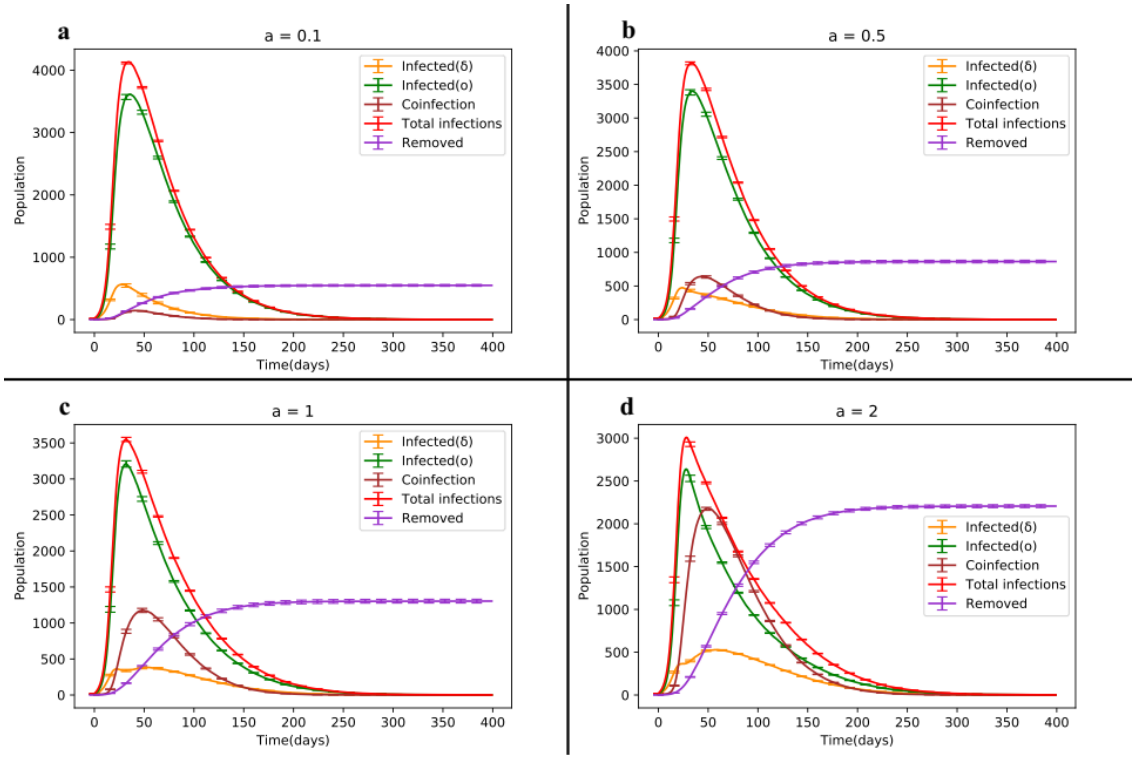

Fig 6. Dynamic changes diagram of the SIRS model illustrating the competition between different variants of Covid-19 for different coefficients of a in the coinfection state.

With an increase in the coefficient a_i, a remarkable rise in the dynamics of the coinfection class is observed. Additionally, the dynamics of susceptible individuals decrease, as illustrated in Figure 7.

Table 3. Statistics of SIRS model results, for four coinfection state of Deltacron

State	Description	a=0.1	a=0.5	a=1	a=2
I_{1max}	Peak domain of dynamics of infected individuals to strain 1	562	476	385	529
I_{2max}	Peak domain of dynamics of infected individuals to strain 2	3611	3400	3208	2640
I_{12max}	Peak domain of dynamics of co-infected individuals to strain 12	145	644	1177	2181
I_{1avg}	The total mean of dynamics of infected individuals to strain 1	80	92	108	159
I_{2avg}	The total mean of dynamics of infected individuals to strain 2	672	642	598	487
I_{12avg}	The total mean of dynamics of co-infected individuals to strain 12	20	104	218	445
S_{min}	The minimum value of dynamics of susceptible individuals at the peak of the disease	5569	5390	5232	4777
Total Infected	The total stats of infected individuals to disease	10744	13294	16737	23459
Total Recovered	The total stats of recovered individuals from disease	10137	12083	14694	19779
Total Removed due to infection	The total stats of removed individuals from disease	5490	864	1304	2206

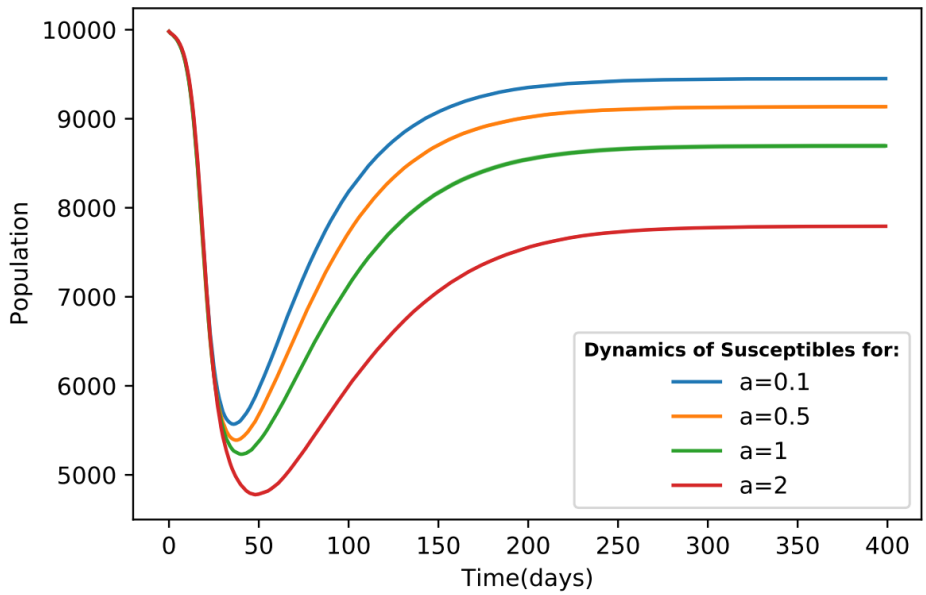

Fig 7. Dynamic changes of susceptible individuals in four different scenarios of Deltacron outbreak.

3.4. The impact of topology

This section explores the influence of network topology on the dynamics of infection spreading. In addition to the previously discussed Erdős-Rényi (ER) network, we now investigate the Barabási-Albert (BA) and Watts-Strogatz (WS) networks to understand the competition between the Omicron and Delta variants, as well as the coinfection state involving these two strains.

We examine the performance of the model on the WS network with different rewiring probabilities: P = 0 (representing the regular state), P = 0.1 (exhibiting small-world features) and P = 1 (representing the random state). This analysis encompasses both the single infection and coinfection models.

Despite the heterogeneity and the presence of a hub in the BA network (due to the limited network size), the results associated with this network structure align with those observed in the ER random network and the WS random state. Figure 8 illustrates that no significant differences are discernible, with the average total disease proportion in parts c and d being equal to 7.55%.

The average ratio of the clustering coefficient to the average path length in parts a, b and c is 0.001, 0.08 and 0.0002, respectively. Furthermore, the average total disease proportions for cases a, b and c are 0.64%, 7.47% and 7.55%, respectively. The larger average path length in case a contributes to a mortality rate that is 3.2 times higher than that observed in the other two cases. By comparing these three states, we find that the regular state of the WS network exhibits a smaller disease prevalence throughout the epidemic.

The primary distinction between states b and c lies in the infection peak time for each strain. Although the curves in these two states are almost identical, the small-world feature causes infections to occur later. The formation of clusters in the network leads to a higher prevalence of single-strain infections compared to coinfections. Conversely, in the random state, the occurrence of two-strain infections is more widespread, resulting in earlier infections among nodes. As depicted in Figure 9, the difference in the trough point of susceptible individuals dynamics for part b compared to the WS random network is 5.38% and this drop occurs 22 days later than in the random state.

All three states b, c and d exhibit similar disease prevalence. Therefore, at the end of the epidemic, they converge to the same equilibrium point in Figure 9. Compared to the regular case, the difference in the equilibrium state is approximately 3%, indicating that the number of removed individuals is around 300 higher in the random network than in the regular network.

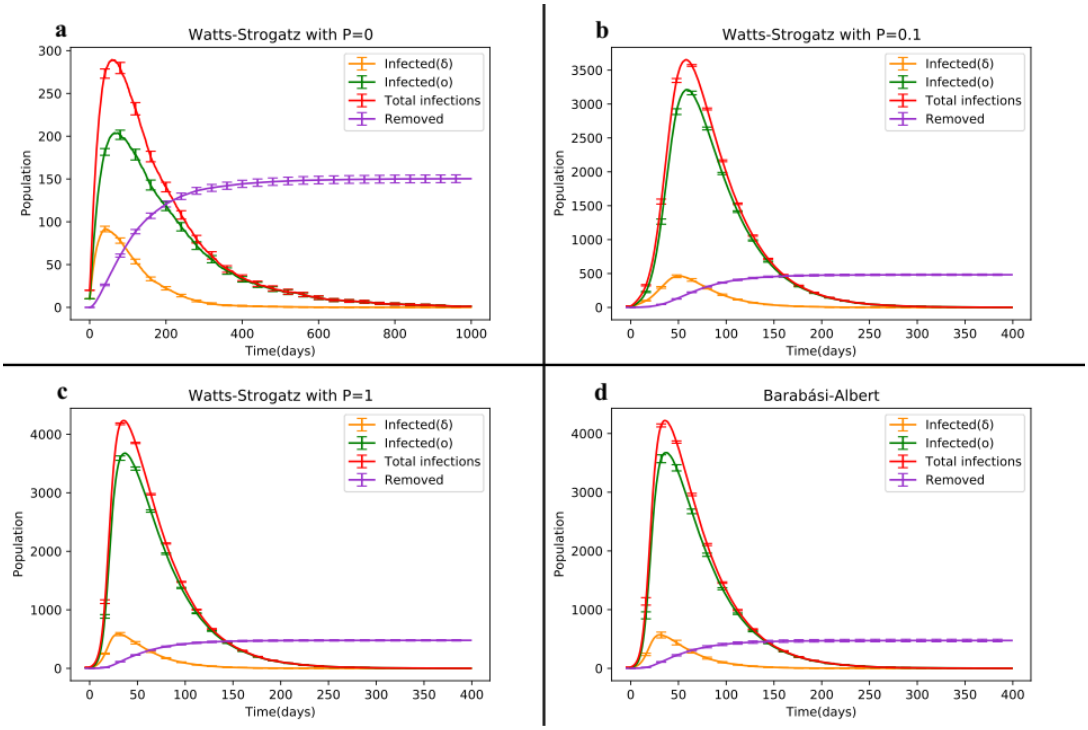

Fig 8. Dynamic changes of the SIRS model depicting the competition between Delta and Omicron strains in the Barabasi-Albert (BA) and Watts-Strogatz (WS) network structures.

The coinfection state of the four aforementioned network structures is depicted in Figure 10. It is evident that the average number of dynamically co-infected individuals in the WS network with P=0 is negligible compared to the other structures. In part b (representing the small-world network), the average total disease prevalence is approximately 0.2% higher than in the two random cases, c and d. However, the average coinfection rate in part b is only half of that observed in the random cases. This reduced occurrence of strain coexistence represents the main difference between part b and the random states, c and d.

As shown in Figure 10 (b, c and d), the mortality caused by Deltacron is higher than that caused by both the Delta and Omicron strains. Additionally, the mortality resulting from coinfection

in part b is roughly half of that observed in the random states. Recent explanations indicate that Deltacron exhibits significantly higher virulence.

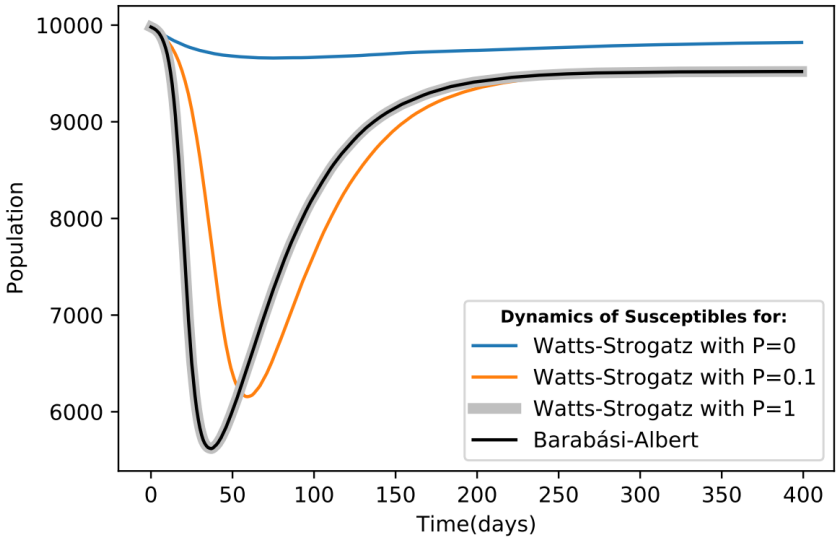

Fig 9. Dynamic changes of susceptible individuals in the Watts-Strogatz (WS) and Barabasi-Albert (BA) network structures for three different states.

In accordance with Figure 3-d, the Delta strain, known for its high severity and wide range of diseases and mortality, diminishes from the epidemic scene when the Omicron strain is present. This disappearance of the dangerous Delta and Deltacron strains occurs within approximately 250 days, resulting in a reduced disease prevalence.

Table 4. Summary statistics from the SIRS model showcasing the competition between various strains of Covid-19 across different network structures.

state	Description	WS(P=0)	WS(P=0.1)	WS(P=1)	ER	BA
I_{1max}	Peak domain of dynamics of infected individuals to strain 1	91	463	587	513	571
I_{2max}	Peak domain of dynamics of infected individuals to strain 2	204	3212	3677	3735	3674
I_{1avg}	The total mean of dynamics of infected individuals to strain1	13	81	80	70	79
I_{2avg}	The total mean of dynamics of infected individuals to strain 2	51	665	676	685	671
S_{min}	The minimum value of dynamics of susceptible individuals at the peak of the disease	9660	6156	5618	5642	5637
$t_{max}(\delta)$	The time of culminated dynamics of infected individuals to Delta strain	40	51	30	30	30
$t_{max}(o)$	The time of culminated dynamics of infected individuals to Omicron strain	66	59	37	37	37
Total Infected	The total stats of infected individuals to disease	2175	10049	10156	10150	10097
Total Recovered	The total stats of recovered individuals from disease	2025	9565	9677	9698	9622
Total Removed due to infection	The total stats of removed individuals from disease	150	482	479	451	474

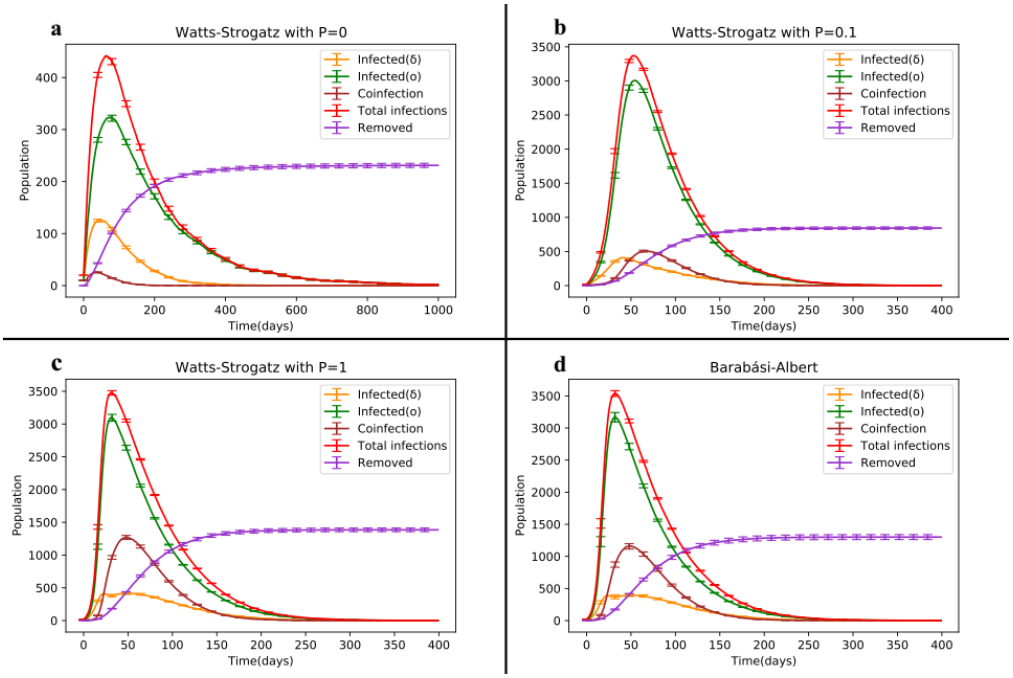

Fig 10. Temporal evolution of the SIRS model in the coinfection state of Delta and Omicron strains, comparing the network structures of Barabasi-Albert (BA) and Watts-Strogatz (WS).

Table 5. Summary statistics of the results obtained from the SIRS model for the coinfection strain Deltacron across different network structures.

State	Description	WS(P=0)	WS(P=0.1)	WS(P=1)	ER	BA
I_{1max}	Peak domain of dynamics of infected individuals to strain 1	125	409	416	385	398
I_{2max}	Peak domain of dynamics of infected individuals to strain 2	324	3006	3098	3208	3167
I_{12max}	Peak domain of dynamics of co-infected individuals to strain 12	26	506	1269	1177	1159
I_{1avg}	The total mean of dynamics of infected individuals to strain 1	17	89	118	108	112
I_{2avg}	The total mean of dynamics of infected individuals to strain 2	77	636	584	598	592
I_{12avg}	The total mean of dynamics of co-infected individuals to strain 12	2	100	235	218	215
S_{min}	The minimum value of dynamics of susceptible individuals at the peak of the disease	9452	5923	5178	5232	5240
$t_{max}(\delta)$	The time of culminated dynamics of infected individuals to Delta strain	44	42	51	51	51
$t_{max}(o)$	The time of culminated dynamics of infected individuals to Omicron strain	76	54	31	32	32
$t_{max}(\text{Deltacron})$	The time of culminated dynamics of infected individuals to Deltacron	35	68	48	49	49
Total Infected	The total stats of infected individuals to disease	3414	13085	17258	16737	16631
Total Recovered	The total stats of recovered individuals from disease	3172	11907	15075	14694	14606
Total Removed	The total stats of removed individuals from disease	201	843	1385	1304	1301

The abundance of infected individuals to the Delta and Omicron strains for their first, second, third and fourth occurrences is displayed. As the Omicron strain exhibits dominance, the number of engagements with this strain surpasses that of the Delta strain and spans a wider range. In the WS network with a rewiring probability of P=0.1 (small-world feature), the prevalence domain of the Delta strain is nearly equivalent to that of the random networks for the first occurrence of infection, while it doubles for the second occurrence. This difference can be attributed to the substantial clustering observed in the small-world network.

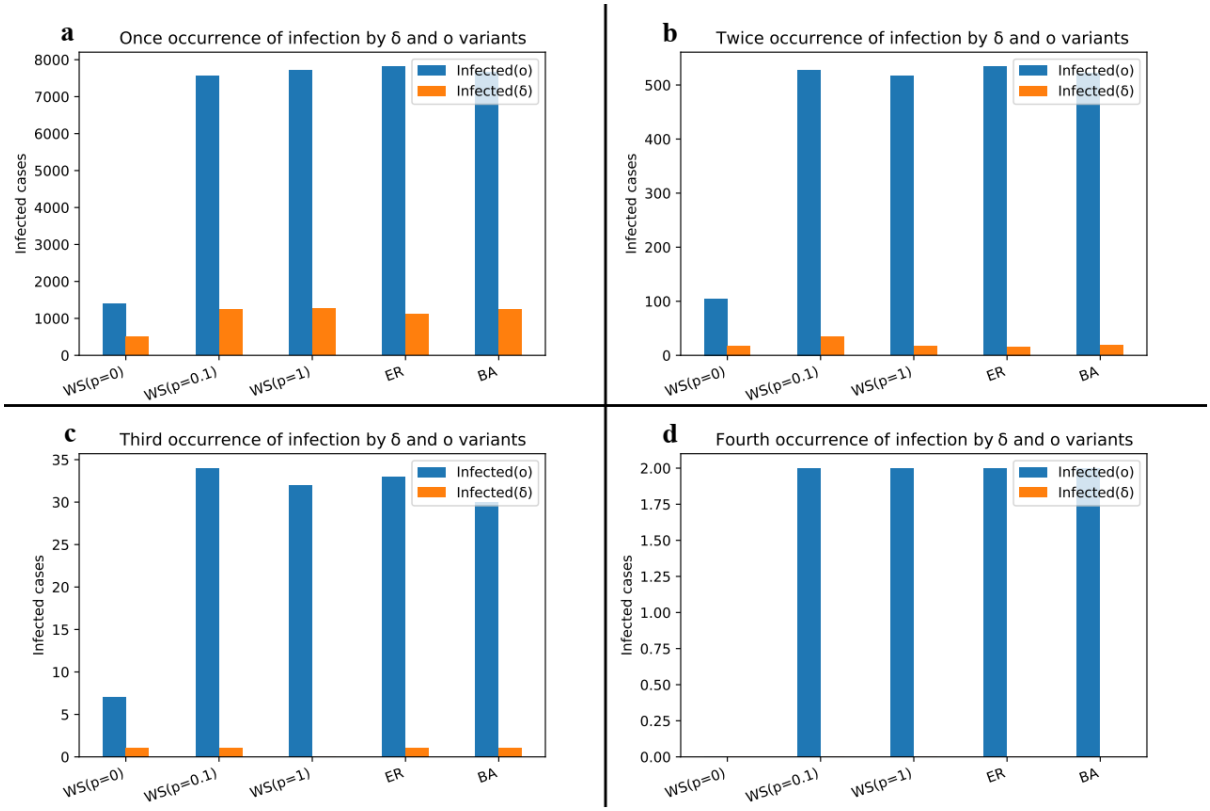

Fig 11. Bar plot depicting the cumulative count of individuals experiencing multiple infections by the Delta and Omicron strains in the competitive model.

In the coinfection model (refer to Figure 12), the Omicron strain exhibits progression up to the third occurrence and during the second and third occurrences, the WS network with a rewiring probability of P=0.1 generates a larger domain compared to the random networks. Moreover, the prevalence of the coinfection state in this network is significantly lower than in random networks. This discrepancy arises from the fact that networks with a small-world feature exhibit a higher average ratio of clustering coefficient to average path length compared to random networks. Consequently, numerous clusters form within the small-world network, resulting in a higher prevalence of single infections within these clusters. As a result, individuals infected with one strain are less likely to encounter the second strain within their local neighborhood, leading to a lower incidence of coinfection. In random networks, however, the distribution of both strains is more random throughout the network, promoting a more widespread occurrence of coinfection in the homogeneous Erdős-Rényi network (characterized

by greater randomness) and the heterogeneous Barabasi-Albert network (featuring the presence of hubs).

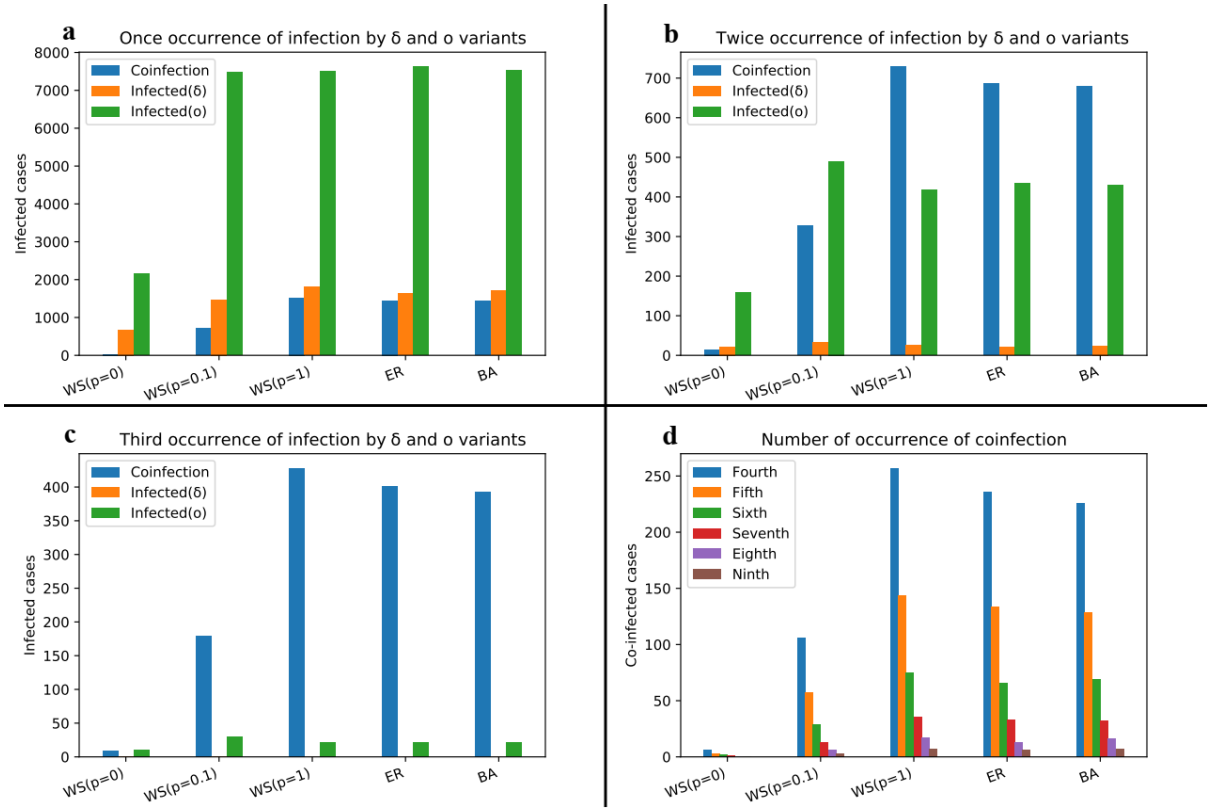

Fig 12. Bar chart illustrating the cumulative count of individuals infected multiple times by the Delta, Omicron and Deltacron strains in the coinfection model.

4. Conclusion

This study comprehensively investigated two epidemic models, focusing on single infection and coinfection scenarios to examine the dynamics of multi-infectious models. The Alpha and Beta strains, characterized by higher transmissibility, contributed to a larger epidemic range. Moreover, the Delta strain emerged as significantly more virulent and invasive than previous strains, warranting major concern.

Among the Variants of Concern (Omicron, Alpha, Beta, Gamma and Delta), the relatively less virulent Omicron strain assumed a dominant role and became the primary focus of investigation. Its interactions with other Variants of Concern were explored across random networks and various social network structures. In each case, Omicron exhibited superior competitive advantage, leading to its widespread prevalence in society. By effectively displacing the more virulent strains, Omicron prevented further transmission of infections and facilitated the transition of infected individuals into the removed class.

This dominance of the Omicron strain is prominently evident in the delayed state, where its introduction as the secondary strain gradually diminished the prevalence of more virulent strains. Remarkably, Omicron acted akin to a vaccine by swiftly suppressing the dangerous strain within the population.

Furthermore, in the coinfection state within the Erdős-Rényi (ER) network, an increase in the coinfection coefficient (a) corresponded to an escalation in the dynamics of coinfection individuals, while the dynamics of infected individuals to the Delta strain diminished over time. When analyzing the impact of network topology, it became apparent that the high ratio of average clustering coefficient to average path length in the Watts Strogatz (WS) network with small-world features, in comparison to random and Barabasi-Albert (BA) networks, resulted in a reduced occurrence of coinfection. This can be attributed to the formation of clusters predominantly hosting single infections and having fewer neighboring individuals infected with the second strain within their adjacency.

In summary, this research sheds light on the dynamics of epidemic models, highlighting the dominance of the Omicron strain as a less virulent yet highly competitive variant. The findings underscore the efficacy of Omicron in supplanting more virulent strains and its potential role in mitigating the spread of infectious diseases. The study also emphasizes the influence of network topology on the occurrence of coinfection, with the small-world structure exhibiting distinct characteristics that limit the prevalence of simultaneous infections. These insights contribute to our understanding of epidemic dynamics and can inform strategies for disease control and prevention.

References:

1. Bull, J.J.J.E., *Virulence.* 1994. **48**(5): p. 1423-1437.
2. Levin, S. and D.J.T.A.N. Pimentel, *Selection of intermediate rates of increase in parasite-host systems.* 1981. **117**(3): p. 308-315.
3. Nowak, M.A. and R.M.J.P.o.t.R.S.o.L.S.B.B.S. May, *Superinfection and the evolution of parasite virulence.* 1994. **255**(1342): p. 81-89.
4. May, R.M. and M.A.J.P.o.t.R.S.o.L.S.B.B.S. Nowak, *Coinfection and the evolution of parasite virulence.* 1995. **261**(1361): p. 209-215.
5. van Baalen, M. and M.W. Sabelis, *The dynamics of multiple infection and the evolution of virulence.* The American Naturalist, 1995. **146**(6): p. 881-910.
6. He, X., et al., *SARS-CoV-2 Omicron variant: characteristics and prevention.* 2021. **2**(4): p. 838-845.
7. Vasireddy, D., et al., *Review of COVID-19 variants and COVID-19 vaccine efficacy: what the clinician should know?* 2021. **13**(6): p. 317.
8. V'kovski, P., et al., *Coronavirus biology and replication: implications for SARS-CoV-2.* 2021. **19**(3): p. 155-170.
9. Chen, B., et al., *Overview of lethal human coronaviruses.* 2020. **5**(1): p. 89.
10. Zhao, Y., et al., *The global transmission of new coronavirus variants.* 2022. **206**: p. 112240.
11. Greaney, A.J., et al., *Comprehensive mapping of mutations in the SARS-CoV-2 receptor-binding domain that affect recognition by polyclonal human plasma antibodies.* 2021. **29**(3): p. 463-476. e6.
12. Choi, J.Y. and D.M.J.Y.m.j. Smith, *SARS-CoV-2 variants of concern.* 2021. **62**(11): p. 961.
13. CDC. *Science Brief: Emerging SARS-CoV-2 Variants*. Jan 28, 2021. [Accessed on July 9, 2022]; Available from: https://www.cdc.gov/coronavirus/2019-ncov/science/science-briefs/scientific-brief-emerging-variants.html#ref2.
14. HIV, C.I. *Wild-Type Virus*. [Accessed on July 9, 2022]; Available from: https://clinicalinfo.hiv.gov/en/glossary/wild-type-virus.

15. Chatterjee, S., et al., *Studying the progress of COVID-19 outbreak in India using SIRD model.* 2021. **95**: p. 1941-1957.
16. Lin, L., et al., *The disease severity and clinical outcomes of the SARS-CoV-2 variants of concern.* 2021. **9**: p. 775224.
17. Islam, S., T. Islam, and M.R.J.C.p. Islam, *New coronavirus variants are creating more challenges to global healthcare system: a brief report on the current knowledge.* 2022. **15**: p. 2632010X221075584.
18. Davies, N.G., et al., *Estimated transmissibility and impact of SARS-CoV-2 lineage B. 1.1. 7 in England.* 2021. **372**(6538): p. eabg3055.
19. Tang, J.W., P.A. Tambyah, and D.S.J.J.o.I. Hui, *Emergence of a new SARS-CoV-2 variant in the UK.* 2021. **82**(4): p. e27-e28.
20. Lang, K.J.M.N.T., *Delta Variant has 235% Higher Risk of ICU Admission than Original Virus.* 2021. **8**.
21. Shiehzadegan, S., et al., *Analysis of the delta variant B. 1.617. 2 COVID-19.* 2021. **11**(4): p. 778-784.
22. Bolze, A., et al., *SARS-CoV-2 variant Delta rapidly displaced variant Alpha in the United States and led to higher viral loads.* 2022. **3**(3).
23. de León, U.A.-P., et al., *Modeling COVID-19 dynamic using a two-strain model with vaccination.* 2022. **157**: p. 111927.
24. Tegally, H., et al., *Detection of a SARS-CoV-2 variant of concern in South Africa.* 2021. **592**(7854): p. 438-443.
25. Silva, J.P., et al., *Delta variant of SARS-CoV-2 replacement in Brazil: a national epidemiologic surveillance program.* 2022. **14**(5): p. 847.
26. Coutinho, R.M., et al., *Model-based estimation of transmissibility and reinfection of SARS-CoV-2 P. 1 variant.* 2021. **1**(1): p. 48.
27. SARS-CoV, P.J.P.H.E., London, *variants of concern and variants under investigation in England–technical briefing 15.* 2021.
28. FEHV. *Characteristics of Delta coronavirus variant*. July 11, 2021 [Accessed on july 9, 2022]; Available from: https://fehv.org/en/characteristics-delta-coronavirus-variant/.
29. Araf, Y., et al., *Omicron variant of SARS-CoV-2: genomics, transmissibility, and responses to current COVID-19 vaccines.* 2022. **94**(5): p. 1825-1832.
30. Yang, W. and J.J.m. Shaman, *SARS-CoV-2 transmission dynamics in South Africa and epidemiological characteristics of the Omicron variant.* 2021: p. 2021.2012. 2019.21268073.
31. Lewnard, J.A., et al., *Clinical outcomes among patients infected with Omicron (B. 1.1. 529) SARS-CoV-2 variant in southern California.* 2022: p. 2022.01. 11.22269045.
32. Cantón, R., et al., *New variants of SARS-CoV-2.* 2021. **34**(5): p. 419.
33. Grint, D.J., et al., *Case fatality risk of the SARS-CoV-2 variant of concern B. 1.1. 7 in England, 16 November to 5 February.* 2021. **26**(11): p. 2100256.
34. WHO. *Tracking SARS-CoV-2 variants*. 2022 [Accessed on July 9, 2022]; Available from: https://www.who.int/activities/tracking-SARS-CoV-2-variants.
35. He, Y., et al., *Possible recombination between two variants of concern in a COVID-19 patient.* 2022. **11**(1): p. 552-555.
36. Maulud, S.Q., et al., *Deltacron: Apprehending a new phase of the COVID-19 pandemic.* 2022. **102**: p. 106654.
37. Ou, J., et al., *Tracking SARS-CoV-2 Omicron diverse spike gene mutations identifies multiple inter-variant recombination events.* 2022. **7**(1): p. 138.
38. Mandal, M., et al., *A model based study on the dynamics of COVID-19: Prediction and control.* 2020. **136**: p. 109889.
39. Pharaon, J. and C.T.J.J.o.t.b. Bauch, *The influence of social behaviour on competition between virulent pathogen strains.* 2018. **455**: p. 47-53.

40. Anastassopoulou, C., et al., *Data-based analysis, modelling and forecasting of the COVID-19 outbreak.* 2020. **15**(3): p. e0230405.
41. Miró Pina, V., et al., *The role of connectivity on COVID-19 preventive approaches.* 2022. **17**(9): p. e0273906.
42. Hernández, P., et al., *A new formulation of compartmental epidemic modelling for arbitrary distributions of incubation and removal times.* 2021. **16**(2): p. e0244107.
43. Mosquera, J. and F.R.J.J.o.T.B. Adler, *Evolution of virulence: a unified framework for coinfection and superinfection.* 1998. **195**(3): p. 293-313.
44. Wang, Y., et al., *Reduction of secondary transmission of SARS-CoV-2 in households by face mask use, disinfection and social distancing: a cohort study in Beijing, China.* 2020. **5**(5): p. e002794.
45. Bourouiba, L.J.J., *Turbulent gas clouds and respiratory pathogen emissions: Potential implications for reducing transmission of COVID-19.* 2020. **323**(18): p. 1837-1838.
46. Leung, N.H., et al., *Respiratory virus shedding in exhaled breath and efficacy of face masks.* 2020. **26**(5): p. 676-680.
47. Guo, Y., et al., *Factors influencing social distancing to prevent the community spread of COVID-19 among Chinese adults.* 2021. **143**: p. 106385.
48. Calafiore, G.C., C. Novara, and C. Possieri. *A modified SIR model for the COVID-19 contagion in Italy*. in *2020 59th IEEE Conference on Decision and Control (CDC)*. 2020. IEEE.
49. Samui, P., et al., *A mathematical model for COVID-19 transmission dynamics with a case study of India.* 2020. **140**: p. 110173.
50. Danane, J., et al., *Mathematical analysis and simulation of a stochastic COVID-19 Lévy jump model with isolation strategy.* 2021. **23**: p. 103994.
51. Mwalili, S., et al., *SEIR model for COVID-19 dynamics incorporating the environment and social distancing.* 2020. **13**(1): p. 1-5.
52. Ahmad, Z., et al., *A report on COVID-19 epidemic in Pakistan using SEIR fractional model.* 2020. **10**(1): p. 22268.
53. Okuonghae, D., A.J.C. Omame, Solitons, and Fractals, *Analysis of a mathematical model for COVID-19 population dynamics in Lagos, Nigeria.* 2020. **139**: p. 110032.
54. Olaniyi, S., et al., *Mathematical modelling and optimal cost-effective control of COVID-19 transmission dynamics.* 2020. **135**(11): p. 938.
55. Biswas, S.K., et al., *COVID-19 pandemic in India: a mathematical model study.* 2020. **102**: p. 537-553.
56. Das, S., et al., *Is Omicron the end of pandemic or start of a new innings?* 2022: p. 102332.
57. Yadav, P.D., et al., *Substantial immune response in Omicron infected breakthrough and unvaccinated individuals against SARS-CoV-2 variants of concern.* 2022. **84**(5): p. e80-e81.